The Journal of Immunology

RESEARCH ARTICLE | JANUARY 03 2024

A Lipopolysaccharide-Enriched Cow's Milk Allergy Microbiome Promotes a TLR4-Dependent Proinflammatory Intestinal Immune Response

Evelyn Campbell; ... et. al

J Immunol (2024) 212 (4): 702–714.
https://doi.org/10.4049/jimmunol.2300518

A Lipopolysaccharide-Enriched Cow's Milk Allergy Microbiome Promotes a TLR4-Dependent Proinflammatory Intestinal Immune Response

Evelyn Campbell,* Lauren A. Hesser,[†,‡] Roberto Berni Canani,[§] Laura Carucci,[§] Lorella Paparo,[§] Robert T. Patry,[†] and Cathryn R. Nagler[†,‡]

We have previously reported that the gut microbiota of healthy infants harbors allergy-protective bacteria taxa that are depleted in infants with cow's milk allergy (CMA). Few reports have investigated the role of the gut microbiota in promoting allergic responses. In this study we selected a CMA-associated microbiota with increased abundance of Gram-negative bacteria for analysis of its proinflammatory potential. LPS is the major component of the outer membrane of Gram-negative bacteria. Colonization of mice with a global or conditional mutation of the LPS receptor TLR4 with this CMA microbiota induced expression of serum amyloid A1 (*Saa1*) and other Th17-, B cell–, and Th2-associated genes in the ileal epithelium in a TLR4-dependent manner. In agreement with the gene expression data, mice colonized with the CMA microbiota have expanded populations of Th17 and regulatory T cells and elevated concentrations of fecal IgA. Importantly, we used both antibiotic-treated specific pathogen-free and germ-free rederived mice with a conditional mutation of TLR4 in the CD11c^{+} compartment to demonstrate that the induction of proinflammatory genes, fecal IgA, and Th17 cells is dependent on TLR4 signaling. Furthermore, metagenomic sequencing revealed that the CMA microbiota has an increased abundance of LPS biosynthesis genes. Taken together, our results show that a microbiota displaying a higher abundance of LPS genes is associated with TLR4-dependent proinflammatory gene expression and a mixed type 2/type 3 response in mice, which may be characteristic of a subset of infants with CMA. ***The Journal of Immunology*, 2024, 212: 702–714.**

In the last 30 y, food allergies (FAs), along with asthma, eczema, and other atopic diseases, have become more common in the United States and other first-world countries (1, 2). FAs can present with a multitude of symptoms, such as hives, itchy throat, wheezing, difficulty breathing, vomiting, and life-threatening anaphylactic shock. Therapeutic interventions remain limited, and FAs are a growing global public health concern (3, 4). The generational increase in FAs coincides with Western lifestyle factors including consumption of highly processed foods low in dietary fiber, overuse of antibiotics, and cesarean birth that have, collectively, contributed to gut dysbiosis (5). Numerous epidemiological studies report direct correlations between neonatal antibiotic-driven microbial perturbation and atopic diseases (6–8), adding to increasing evidence that early life immunological education is regulated by microbial exposure and can impact susceptibility to inflammatory diseases later in life.

Work from our laboratory, and others, has demonstrated in murine models that intestinal bacteria regulate allergic responses to food (9–14). Initial translational studies showed that the fecal microbiota of infants with cow's milk allergy (CMA) is distinct from that of healthy infants in demographically matched cohorts (15). To establish a gnotobiotic model of CMA we transferred fecal bacterial communities from four infants with CMA and four healthy infants into germ-free (GF) mice and sensitized them to a major cow's milk allergen, β-lactoglobulin (BLG) (12). Upon intragastric challenge with BLG, mice colonized with the healthy infants' microbiota were protected against an anaphylactic response (12). In contrast, mice colonized with the CMA-associated gut microbiota were susceptible to an anaphylactic response and had elevated serum concentrations of BLG-specific IgE and IgG1 compared with GF and healthy-colonized mice (12), suggesting that the CMA microbiota may promote allergic responses to food. De Filippis et al. (16) extended these initial findings by examining the proinflammatory characteristics of the fecal microbiome in a large study of 90 allergic children and 30 age-matched healthy controls from the same demographic cohort at the University of Naples. We were intrigued by the observation that the fecal metagenomes of allergic children were enriched for genes involved in the biosynthesis of LPS (16).

In this study, we selected a CMA microbiota to investigate whether and how TLR4, the receptor for LPS, regulates allergic sensitization to food in a gnotobiotic model. We show that this CMA microbiota induces expression of serum amyloid A1 (*Saa1*) in the ileal epithelium of colonized mice and that elevated concentrations of SAA-1 are detectable in the serum of a subset of patients with CMA. We

*Committee on Microbiology, University of Chicago, Chicago, IL; [†]Department of Pathology, University of Chicago, Chicago, IL; [‡]Pritzker School of Molecular Engineering, University of Chicago, Chicago, IL; and [§]Department of Translational Medical Science and ImmunoNutrition Lab at CEINGE Advanced Biotechnologies Research Center and Task Force for Microbiome Studies, Section of Pediatrics, University of Naples Federico II, Naples, Italy

ORCIDs: 0000-0001-7490-3999 (L.C.); 0000-0001-7254-6617 (C.R.N.).

Received for publication August 2, 2023. Accepted for publication December 12, 2023.

This work was supported by National Institute of Allergy and Infectious Diseases Grant AI146099 (to C.R.N. and E.C.).

The sequencing data presented in this article have been submitted to the National Center for Biotechnology Information Sequence Read Archive under accession numbers PRJNA860615 and PRJNA869952.

Address correspondence and reprint requests to Dr. Cathryn R. Nagler, University of Chicago, Jules F. Knapp Medical Research Building, 924 East 57th Street, JFK 410, Chicago, IL 60637-1824. E-mail address: cnagler@bsd.uchicago.edu

The online version of this article contains supplemental material.

Abbreviations used in this article: BLG, β-lactoglobulin; CMA, cow's milk allergy; CT, cholera toxin; DC, dendritic cell; EHCF, extensively hydrolyzed casein formula; FA, food allergy; FDR, false discovery rate; GF, germ-free; GRAF, Gnotobiotic Research Animal Facility; IEC, intestinal epithelial cell; LP, lamina propria; qRT-PCR, quantitative reverse transcription–PCR; RT, room temperature; SAA-1, serum amyloid A1; SPF, specific pathogen-free; Treg, regulatory T cell; WT, wild-type.

https://doi.org/10.4049/jimmunol.2300518

demonstrate that, in mice colonized with the CMA microbiota, the induction of *Saa1*, regulatory T cells (Tregs), and Th17 cell populations in the ileum is regulated by TLR4 signaling, particularly in $CD11c^+$ cells. Analysis of ileal contents of mice colonized with the CMA microbiota revealed an increased representation of Gram-negative bacteria, particularly Bacteroidetes and Proteobacteria, when compared with mice colonized with the microbiota of a healthy infant. These results illuminate a previously unappreciated role for the TLR4/LPS innate signaling axis as a mechanism by which the CMA-associated dysbiotic gut microbiota contributes to inflammatory responses associated with FAs.

Materials and Methods

Mouse husbandry and care

All mice used in these experiments were housed and bred at the University of Chicago of Animal Resource Center in a specific-pathogen free (SPF) facility or the Gnotobiotic Research Animal Facility (GRAF) under a 12-h light/12-h dark cycle. Mouse cages were autoclaved and bedded with pine shavings. Mice maintained in GRAF were housed in Trexler-style flexible film isolators (Class Biologically Clean) with Ancare polycarbonate mouse cages (catalog no. N10HT). Gnotobiotic mice were fed an autoclaved diet (5K67, Purina Lab Diets; sterilized at 121°C for 30 min). Mice colonized with infant-derived microbiota received sterile extensively hydrolyzed casein formula (EHCF; Nutramigen); GF mice received sterile water ad libitum (12). Cage bedding for gnotobiotic mice was changed daily or every other day due to leakage of formula from the bottles. The sterility of each isolator was confirmed using culture-dependent and culture-independent methods on a weekly basis. Collected fecal pellets were homogenized and cultured in brain–heart infusion, nutrient, and Sabouraud broth at 37 and 42°C under aerobic and anaerobic conditions, respectively, for 96 h. DNA isolated from collected fecal pellets was analyzed for the presence of the 16S rRNA gene as previously described (11). Upon rederivation or acquisition of new animals into the gnotobiotic colony, all mice were screened for parasites, full serology profile, and/or PCR, bacteriology, and gross and histological analysis of major organs through IDEXX Radil or Charles River Laboratories using an Axenic profile screen. SPF mice were fed an irradiated standard chow diet (Teklad 2916, Envigo) and water ad libitum. All experiments were performed in compliance with the University of Chicago Animal Care and Use protocols.

Mouse lines

SPF C57BL/6 $CD11c^{cre}$ and C56BL/6 $Tlr4^{fl/fl}$ mice were purchased from The Jackson Laboratory. C57BL/6 $CD11c^{cre}$ and $Tlr4^{fl/fl}$ mice were bred in-house to obtain a $CD11c^{cre}Tlr4^{fl/fl}$ colony. SPF wild-type (WT) $Foxp3^{GFP}$ and $Tlr4^{-/-}Foxp3^{GFP}$ mice, both on a C57BL/6J background, were bred in-house. C57BL/6 $Foxp3^{GFP}$ mice were crossed with $Tlr4^{-/-}$ mice (originally from The Jackson Laboratory) to create a homozygous mutant colony. C57BL/6 $Foxp3^{GFP}$ and C57BL/6 $Tlr4^{-/-}Foxp3^{GFP}$ mice were rederived GF by Kathy McCoy at McMaster University (Hamilton, ON, Canada) as previously reported (11). The conditional mutant $CD11c^{cre}Tlr4^{fl/fl}$ mice were rederived GF by Kathy McCoy at the University of Calgary International Microbiome Center (Calgary, AB, Canada). GF C3H/HeN, C57BL/6 $Foxp3^{GFP}$, $Tlr4^{-/-}Foxp3^{GFP}$ and $CD11c^{cre}Tlr4^{fl/fl}$ mice were maintained in flexible film gnotobiotic breeding isolators in GRAF. $Tlr4^{-/-}Foxp3^{GFP}$ were bred as homozygous mutants. $CD11c^{cre}Tlr4^{fl/fl}$ mice were bred as heterozygotes ($CD11c^{cre+/-}Tlr4^{fl/fl} \times CD11c^{cre-/-}Tlr4^{fl/fl}$). Each experiment was littermate controlled.

Colonization of experimental mice with the human infant gut microbiota

Human infant microbiota repository mice were originally created by intragastrically gavaging C3H/HeN mice with 500 μl of prepared human infant fecal homogenate at weaning as described (12). Repository mice for each donor were housed in separate isolators to avoid microbial cross-contamination. Fecal samples from both repository and experimental mice were routinely examined by 16S rRNA sequencing analysis, which demonstrated that mouse-to-mouse transfer from repository to experimental mice by intragastric gavage of feces was highly reproducible and stable over time.

For colonization experiments GF mice were gavaged intragastrically at weaning with 250 μl of feces freshly obtained from CMA or healthy repository mice and homogenized in PBS. Prior to colonization, mice were fed the EHCF (Nutramigen) formula at a 1:4 dilution in water for 4 h to aid in the engraftment of the human infant microbiota. After colonization, both CMA- and healthy-colonized mice were provided diluted EHCF formula. On day 7 postcolonization, mice were euthanized and fecal, cecal, and ileal contents were collected and stored at −20°C.

For SPF mice, littermates were treated intragastrically with 100 μl of an antibiotic mixture of kanamycin sulfate (4 mg/ml), gentamicin sulfate (0.35 mg/ml), colistin sulfate (8500 U/ml), metronidazole (2.15 mg/ml), and vancomycin hydrochloride (0.45 mg/ml) daily for 7 d prior to weaning as described (11). At weaning, mice were colonized by intragastric gavage with 250 μl of freshly homogenized feces obtained from CMA or healthy repository mice. SPF littermate experimental controls followed the same antibiotic treatment regimen but did not receive a fecal gavage at weaning. Mice colonized with the human infant microbiota followed the same experimental timeline as their GF counterparts and were euthanized at 7 d postcolonization. Intestinal contents were stored as previously described.

Sensitization of mice with BLG

For a sensitization model abbreviated from what has been previously reported (12), mice were colonized at weaning with either the CMA or healthy microbiota. Mice were sensitized at 2, 4, 6, and 8 d postweaning with 20 mg of BLG and 10 μg of cholera toxin (CT). Mice were euthanized on day 15 postweaning and spleens were collected and processed into single-cell suspensions. Splenocytes were stimulated in vitro with 10 mg/ml BLG, anti-CD3/anti-CD28 (as a positive control), or unstimulated (as a negative control). For positive controls, culture plates were pretreated with anti-CD3 (1 μg/ml) in PBS for 2 h at room temperature (RT). PBS was aspirated off and cells were cultured in 10 μg/ml anti-CD28. Across all conditions, samples were cultured at a concentration of 2×10^6 cells/ml for 48 h at 37°C/5% CO_2 in DMEM containing 10% FCS, 10 mM HEPES, 100 U/ml penicillin/streptomycin, and 55 μM 2-ME. Cytokines were measured in 48-h culture supernatants by ELISA (IL-13, Invitrogen; IL-17, BioLegend).

Ileal epithelial cell isolation

At euthanasia, whole terminal ileum tissue (measured 10 cm proximal to the cecum) was carefully removed. Ileal tissues were cleaned, inverted, and inflated with enough air to expand the tissue but not rupture it (17). Peyer's patches were not removed. Intestinal epithelial cells were collected from the inflated inverted tissue in cell recovery solution (Corning) by agitating the tissue every 5 min for 30 min on ice. After removing epithelial cells, the remaining lamina propria (LP) tissue was either placed directly into RNAlater (Sigma-Aldrich), incubated at 4°C for 24 h, and stored at −80°C for later analysis, or intestinal lymphocytes were immediately isolated for flow cytometry. Epithelial cells were centrifuged at 800 × *g* for 5 min, lysed in 1 ml of TRIzol reagent (Thermo Fisher Scientific), and stored at −80°C for at least 24 h. RNA from epithelial cells and LP tissue was extracted using the PureLink RNA mini kit according to manufacturer's instructions (Invitrogen). RNA quality and quantity were immediately determined using NanoDrop One (Thermo Scientific). Samples were stored at −80°C until used for cDNA synthesis or RNA sequencing.

Lymphocyte isolation from ileal tissue

Ileal lymphocytes were isolated according to published protocols, with some modification (18, 19). At euthanasia, ileal tissue was cleaned with 1× PBS with mesenteric fat removed and cut longitudinally. The whole tissue was placed into 4 ml of 30 mM EDTA and 1.5 mM DTT in 1× PBS for 20 min on ice. The tissue was then transferred to 4 ml of 30 mM EDTA in 1× PBS and incubated for 10 min at 37°C, followed by gentle shaking for 30 s. Tissues were then transferred to a six-well plate and washed with 10 ml of 1× PBS to remove the remaining epithelial cells. In studies analyzing T cell subsets, tissues were transferred to a 3-ml digest solution of DMEM with 4% FCS containing 40 μg/ml DNAse and 0.5 mg/ml collagenase D (Roche), 0.5 mg/ml Dispase (Roche), or 0.05 mg/ml Liberase (Roche). The tissue was minced finely in the digest solution with surgical scissors and placed into a shaking incubator for 30 min at 37°C, 200 rpm. Following digestion, the cell suspensions were poured over a 70-μm cell strainer into a 50-ml conical tube and washed with 20 ml of 4% FCS in PBS. The cell suspension was spun at 800 × *g* for 5 min and resuspended in 4 ml of RPMI 1640/4% FCS. Next, 4 ml of 80% Percoll was added to the suspension (final 40% Percoll) and the suspension was gently overlaid onto 5 ml of 80% Percoll. The Percoll gradient was centrifuged at 1200 × *g* for 35 min with 0 acceleration and 0 brake deceleration. Cells were collected at the interface of the Percoll layers and washed with 30 ml of DMEM/4% FCS. The cells were then centrifuged at 800 × *g* for 5 min, resuspended in cold DMEM/4% FCS, and counted for viability with trypan blue.

Cell stimulation and staining for flow cytometry

For the staining of T cell subsets, ileal lymphocytes were plated at a concentration of 1×10^6 viable cells/ml in a stimulation solution containing 50 ng/ml PMA (Sigma-Aldrich) and 750 ng/ml ionomycin (Sigma-Aldrich) in the

presence of brefeldin A (10 μg/ml, Sigma-Aldrich). Cells were incubated for 4 h at 37°C, 5% CO_2. After stimulation, cells were centrifuged at 800 × *g* for 5 min and washed in 200 μl of PBS/4% FCS for staining in a 96-well round-bottom plate. Cells were washed and then stained for viability 30 min on ice in the dark using LIVE/Dead fixable aqua (Life Technologies) at a 1:500 dilution. Cells were then incubated in Fc block (anti-mouse CD16/32, Bio X Cell) for 10 min on ice, followed by surface staining on ice in the dark for 30 min. Cells were then fixed using the Foxp3/transcription factor staining buffer set (eBioscience), with prepared solutions according to manufacturer's protocol, for 40 min on ice. Fixed cells were then stained intracellularly for 40 min at RT in the dark. Data were collected on the LSRFortessa 4-15 (BD Biosciences) or Aurora spectral flow cytometer (Cytek) and analyzed using FlowJo software (v10.3.2, Becton Dickinson). The Abs used for flow cytometry were as follows: CD4 (RM4-5, BioLegend), CD45 (30-F11, BioLegend), CD3ε (145-2C11, BioLegend), RORγt (Q31-378, BioLegend), Foxp3 (FJK-16s, Invitrogen), IL-17A (TC11-18H10.1, BioLegend), RORγt (B2D, Thermo Fisher Scientific), Foxp3 (FJK-16s, Thermo Fisher Scientific), Gata3 (L50-233, BD Biosciences), TCRβ (H57-597, BioLegend), CD45 (30-511, BD Biosciences), CD90 (30-H12, BD Biosciences), KLRG1 (2F1/KLRG1, BioLegend), lineage (BioLegend), and CD4 (PC61.5, eBioscience).

ELISAs

Venous blood samples (3 ml) were collected from CMA and healthy patients at the University of Naples Federico I. Samples from CMA patients were obtained following diagnosis at a tertiary pediatric allergic center (Pediatric Allergy Program at the Department of Translational Medical Science of the University of Naples Federico II). Samples from healthy patients who had no risk or history of atopic disorders were obtained from participants in a vaccination program at the University of Naples Federico II. Participation of patients in this study was in compliance with the Declaration of Helsinki and approved by the Ethics Committee of the University of Naples Federico I. Written informed consent was obtained from the parents or guardians of all children involved. Serum was obtained by centrifugation for 15 min and stored at −80°C. IgE specific for the nBos d 5 epitope on BLG was quantified using the Thermo Fisher Scientific ImmunoCAP system and was expressed as kU of allergen-specific IgE/l. Serum SAA-1 levels were determined with a human serum amyloid A ELISA kit (Abcam).

Mouse fecal IgA was quantified as previously described (14). ELISA plates were coated overnight with 2 μg/ml goat-anti mouse IgA-UNLB (Southern-Biotech), 50 μl per well. The next day, plates were washed four times with 300 μl of 1× PBS/0.05% Tween 20 and blocked with 200 μl of 3% BSA in PBS for at least 2 h at RT. Fecal pellets were weighed and placed into 0.01% NaN_3 in 1× PBS (1 ml/100 mg of feces). Pellets were vortexed for 5 min and centrifuged for 15 min at 9600 × *g*. A 9-point standard curve was made by conducting serial 1:1 dilutions of 200 ng/ml stock solution of purified mouse IgA, κ isotype (BD Biosciences). Next, 50 ml of each sample and standard was applied to the wells overnight. The following day, plates were washed and 50 μl of secondary Ab goat anti-mouse IgA-AP (alkaline phosphatase) (SouthernBiotech) diluted 1:2500 was applied to each well and incubated for 1 h at RT. After washing, developer (KPL) was applied to the plate at 100 μl per well for up to 30 min. Development was stopped with 100 μl per well of 5% EDTA in water.

Quantitative reverse transcription–PCR

cDNA was synthesized from isolated RNA using the iScript cDNA synthesis kit with a normalized quantity of RNA for each sample according to the manufacturer's instructions (Bio-Rad). Samples were used immediately for quantitative reverse transcription–PCR (qRT-PCR) analysis or stored at −20°C for future use. cDNA reaction mixes were made using the QuantiNova SYBR Green kit (Qiagen) or PowerUp SYBR Green (Applied Biosystems) according to the manufacturers' instructions. Primers used in the reaction mixes are as follows: *Hprt*, forward, 5′-TGAAGAGCTACTGTAATGATCAGTCAAC-3′, reverse, 5′-AGCAAGCTTGCAACCTTAACCA-3′ (20); *Saa1*, forward, 5′-TGTTCACGAGGCTTTCCAAG-3′, reverse, 5′-CCCG AGCATGGAAGTATTTG-3′ (21); *Reg3b*, forward, 5′-ATGGCTCCTAC TGCTATGCC-3′, reverse, 5′-GTGTCCTCCAGGCCTCTTT-3′ (20); *J chain*, forward, 5′-GAACTTTGTATACCATTTGTCAGACG-3′, reverse, 5′-CTG GGTGGCAGTAACAACCT-3′ (22); *Igha*, forward, 5′-CGTCCAAGAAT TGGATGTGA-3′, reverse, 5′-AGTGACAGGCTGGGATGG-3′ (22); *Il13*, forward, 5′-GGAGCTGAGCAACATCACACA-3′, reverse, 5′-GGTCCTG TAGATGGCATTGCA-3′ (23); *Il17a*, forward, 5′-CAGACTACCTCAA CCGTTCCAC-3′, reverse, 5′-TCCAGCTTTCCCTCCGCATTGA-3′ (OriGene, catalog no. MP206724). Gene expression was measured with the QuantStudio 3 instrument (Applied Biosystems). The cycling conditions for the reaction mixture entailed an activation cycle of 50°C for 2 min followed by one cycle of 95°C for 10 min and 40 cycles at 94°C for 20 s, 55°C for 20 s, and 72°C for 50 s. The fluorescent probe was detected in the last step of the cycle. A melt curve was performed at the end of the PCR reaction to confirm the specificity of the PCR product. Relative expression was calculated by determining the ΔΔCt based on expression of the endogenous housekeeping gene (*Hprt*), followed by normalization to the control group (GF, antibiotic-treated SPF, or healthy) within each genotype.

Bulk RNA sequencing and analysis

RNA libraries for total RNA from ileal epithelial cells were prepared and sequenced at the University of Chicago Functional Genomics Core. Libraries were prepared using a TruSeq stranded total library preparation kit with RiboZero human/mouse/rat (Illumina). Samples were sequenced using 50-bp single-end reads chemistry on the HiSeq 2500 instrument. Raw reads were assessed for quality, counted, and aligned to the mm10 reference genome using the Rsubread package (24). All samples had a Phred score of at least 30. Normalization and differential expression analyses between healthy- and CMA-colonized mice were performed using the edgeR package (25). Read counts for each gene were fit to a negative binomial generalized log-linear model. Multiplicity correction was performed by applying the Benjamini–Hochberg method on the *p* values to control for the false discovery rate (FDR = 0.1). Genes with an FDR of <0.05 and a fold change >1.5 or less than −1.5 were plotted as significant. Gene Ontology pathways for genes expressed in $CD11c^{WT}$ and $CD11c^{\Delta TLR4}$ CMA-colonized mice were determined using Metascape (26).

DNA extraction from fecal and ileal contents for 16S sequencing and analysis

DNA was extracted using the QIAamp PowerFecal Pro DNA kit (Qiagen). Released DNA was then isolated according to the manufacturer's protocol. DNA was purified routinely using a spin column filter membrane and quantified using the Qubit 4 fluorometer (Thermo Fisher Scientific). Ileal contents were subjected to DNA isolation using the PowerSoil DNA isolation kit (MO BIO Laboratories) or the QIAamp PowerFecal Pro DNA kit (Qiagen), according to the manufacturers' protocols.

Isolated DNA was sequenced at the Argonne National Laboratory or the Duchossois Family Institute at the University of Chicago. For samples sequenced at Argonne, 16S rRNA gene amplicon sequencing was performed on an Illumina MiSeq instrument. Paired-end reads (151 bp) were generated with 12-bp barcodes. The V4 region of the 16S rRNA gene was amplified using 515F and 806R primers that included sequencer adapter sequences used in the flow cell as described (12). Raw multiplexed reads were provided by the facility and were demultiplexed using qiime2 (v2018.4) (27).

For samples sequenced at the Duchossois Family Institute, sequencing was performed on the Illumina MiSeq platform in the Functional Genomics Facility at the University of Chicago using 2 × 250 paired-end reads, generating 5,000–10,000 reads per sample. The V4–V5 region within the 16S rRNA gene was amplified using the universal bacterial primers 563F (5′-nnnnnnnn-NNNNNNNNNNN-AYTGGGYDTAAA-GNG-3′) and 926R (5′-nnnnnnnn-NNNNNNNNNNN-CCGTCAATTYHT-TTRAGT-3′), where "N" represents a barcode, and "n" is an additional nucleotide added to offset primer sequencing. Amplicons were then purified using a spin column–based method (Qiagen), quantified, and pooled at equimolar concentrations. Illumina sequencing–compatible unique dual index adapters were ligated onto the pools using the QIAseq one-step amplicon library kit (Qiagen). Library quality control was performed using Qubit 4 fluorometer (Thermo Fisher Scientific) and TapeStation (Agilent) and sequenced on Illumina MiSeq platform to generate 2 × 250-bp reads.

For 16S analysis, Dada2 (v1.14) (28) was used for processing raw 16S rRNA reads. The first 180 bp for both forward and reverse reads were trimmed to remove low-quality nucleotides. Taxonomic analysis was determined using the RDP (Ribosomal Database Project) database (29) with a minimum bootstrap confidence score of 50. Multiple sequence alignment was performed using msa (v1.18.0) (30) and ape (v5.3). Dada2 was used to calculate α and β diversity.

Shotgun metagenomics

Libraries were prepared using 100 ng of genomic DNA using the QIAseq FX DNA library kit (Qiagen). DNA was fragmented enzymatically into smaller fragments and the desired insert size was achieved by adjusting fragmentation conditions. Fragmented DNA was end repaired and poly(A) tails were added to the 3′ ends to stage inserts for ligation. During the ligation step, Illumina compatible unique dual index adapters were added to the inserts and the prepared library was PCR amplified. Amplified libraries were cleaned up, and quality control was performed using a TapeStation (Agilent). Sequencing runs were performed on the Illumina NextSeq platform in the Functional Genomics Facility at the University of Chicago using the 2 × 150 paired-end reads cassette.

For metagenomic analysis, quality reads were used in Kraken2 (v2.1.1) for taxonomic classification and to assemble contigs via MEGAHIT (v1.2.9)

(31). Genes were annotated using Prodigal (v2.6.3) (32), and functional annotations were perform using eggnog-emapper (v2.0.1b) (33). A Wilcoxon rank sum test was performed on metagenome assembled genomes identified in healthy- and CMA-colonized mice to determine differentially abundant species.

Statistical analysis

Statistical analyses were performed using GraphPad Prism v9.3.0. The test details are indicated in the figure legends.

Data availability

The 16S rRNA-targeted and metagenomic sequencing raw FastQ data files have been deposited in the NCBI Sequence Read Archive (https://www.ncbi.nlm.nih.gov/sra, accession no. PRJNA860615). RNA sequencing raw FastQ data files have been deposited (accession no. PRJNA869952).

Results

The microbiota from a CMA donor is associated with an intestinal inflammatory response

We previously showed that mice colonized with the fecal microbiota of CMA infants and sensitized to the cow's milk protein BLG exhibited an elevated BLG-specific IgE and IgG1 response compared with GF mice or mice colonized with the microbiota from healthy infants (12). In the current study we selected one CMA infant donor for further mechanistic analysis. This infant, CMA donor 5, experienced urticaria and gastrointestinal symptoms within a few minutes after feeding with cow's milk and presented with gastrointestinal inflammation, as observed by nodular hyperplasia on the intestinal walls of the rectum (Supplemental Fig. 1A). Histological evaluation revealed eosinophilic infiltration within the gastrointestinal tissue, supporting an immunological basis for the symptoms experienced by this patient (Supplemental Fig. 1A). Some mice colonized with the CMA donor 5 microbiota exhibited bloody intestinal contents in the ileum and loose fecal pellets in the colon as observed at euthanasia at 1 wk postcolonization (Supplemental Fig. 1B). This was not observed in mice colonized with feces from any other CMA or healthy donors. In the original publication (12), ileal and colonic tissues were collected from mice colonized with feces from each of the eight infant donors at euthanasia after 4 wk of sensitization with BLG plus CT and at 5–6 mo postcolonization. The tissues were fixed in formalin and stained with H&E or placed in Carnoy's fixative for periodic acid–Schiff staining. A gastrointestinal pathologist examined the stained sections in a blinded fashion and found no evidence of pathology, ruling out an infectious etiology (12). FA is generally considered to be a Th2-dependent, IgE-driven response. To characterize an intestinal inflammatory response associated with an IgE-mediated FA, we chose CMA donor 5 as the focus of this study; all data pertaining to the CMA microbiota are derived from this donor.

An earlier study showed that LPS biosynthesis genes were enriched in fecal samples from allergic patients from the same Neapolitan demographic cohort as CMA donor 5 (16). We found that Gram-negative (LPS-positive) bacteria including Bacteroidales (Bacteroidaceae and Porphyromonadaceae), Veillonellaceae, and Betaproteobacteria (Sutterellaceae) were enriched in the CMA donor 5 microbiota compared with all healthy donors (Fig. 1A). To more broadly understand how the CMA donor 5 microbiota influences the gut mucosa, bulk RNA sequencing was performed on intestinal epithelial cells (IECs) from the ileum of GF mice, mice colonized with the CMA donor 5 microbiota, and mice colonized with the microbiota of healthy infants (donors 1–4) at 1 wk postcolonization. These data, reanalyzed from our previous study (12), consist of an epithelial preparation that includes cells from the Peyer's patches, since they are not excised in the isolation protocol we used (see *Materials and Methods*). Analysis revealed hundreds of genes that were differentially expressed between CMA donor 5–colonized mice and mice colonized with the healthy microbiota or left GF. Many of these genes are involved in numerous immunological processes, including regulation of the epithelial barrier in response to bacterial colonization (*Defa17*, *Defa23*, *Il18*, *Il15*), APC function (*Cd8a*, *Cd83*), B cell responses (*Jchain*, *Fcgrt*), and type 2 responses (*Il13ra1*, *Il33*) (data not shown) (21, 34–36). Additionally, several genes that have previously been associated with a proinflammatory Th17 signature were significantly upregulated in ileal IECs from CMA donor 5–colonized mice compared with healthy-colonized mice. These genes include *Saa1*, *Slc6a14*, *Fut2*, *Reg3g*, and *Reg3b* (Fig. 1B) (37). *Saa1* was of particular interest because it is a well-characterized acute-phase protein expressed during injury and infection (38). Because mice colonized with the CMA donor 5 microbiota have an inflammatory presentation, we hypothesized that *Saa1* induced by the donor 5 microbiota may be a biomarker for a subset of patients with CMA. To determine whether *Saa1* upregulation was induced by the microbiota of other CMA infants, GF mice were colonized with repository feces from CMA donors 5–8, as well as repository feces from healthy donors 1–4, and were euthanized at 1 wk postcolonization. Expression of *Saa1* was induced by colonization with all donor microbiotas compared with GF controls (Fig. 1C). However, mice colonized with the CMA donor 5 microbiota exhibited significantly higher expression of *Saa1* compared with all other CMA donors, all healthy donors, and GF mice. To examine the relevance of SAA-1 expression to human infants, we quantified SAA-1 in the serum of a larger cohort of 30 healthy and 30 CMA pediatric patients. As expected, CMA patients had significantly higher levels of Abs against nBos d 5 (BLG), a diagnostic indicator of CMA, in comparison with healthy controls (Fig. 1D). Interestingly, these infants also had significantly elevated levels of serum SAA-1 compared with healthy individuals (Fig. 1E), suggesting that SAA-1 may be a biomarker of allergy-associated inflammation in a subset of patients with FA.

Saa1 induction in the ileal epithelium of CMA-colonized mice is regulated by TLR4 signaling

After observing microbially induced expression of *Saa1* in the ileal epithelium of CMA donor 5–colonized mice, we hypothesized that intestinal inflammatory responses mediated by SAA-1 might contribute to some of the inflammatory responses seen in FA. SAA-1 can bind LPS (39), and the microbial signature of CMA donor 5 was highly enriched in Gram-negative bacteria (Fig. 1A). We therefore used CMA donor 5–colonized mice as a model to examine the role of TLR4 in regulating ileal expression of *Saa1*. GF C57BL/6 mice with TLR4 sufficiency and deficiency were colonized at weaning with the CMA microbiota or healthy microbiota and euthanized 1 wk later to examine *Saa1* expression in ileal IECs. *Saa1* was significantly upregulated in CMA-colonized mice colonized compared with GF and healthy-colonized mice only when TLR4 was sufficient (Fig. 2A). In addition to *Saa1*, *Reg3b* has previously been associated with a Th17 signature induced by bacterial adherence to the ileal epithelium (37). When we examined the expression of *Reg3b*, we observed that colonization of mice with both the CMA and healthy microbiotas induced significant upregulation of *Reg3b* compared with GF mice (Fig. 2B). However, in the global absence of TLR4 signaling, CMA-colonized mice did not have significant upregulation of *Reg3b* compared with GF mice. Interestingly, healthy-colonized mice still exhibited significant upregulation of *Reg3b* compared with GF and CMA-colonized mice. These results show that TLR4 signaling regulates the expression of *Saa1* and *Reg3b* induced by the CMA microbiota.

Ileal Tregs and Th17 cells are induced by the CMA donor 5 microbiota in a TLR4-dependent manner

Because SAA-1 has previously been implicated in regulating type 3 inflammation (40, 41), TLR4-dependent induction of *Saa1* would

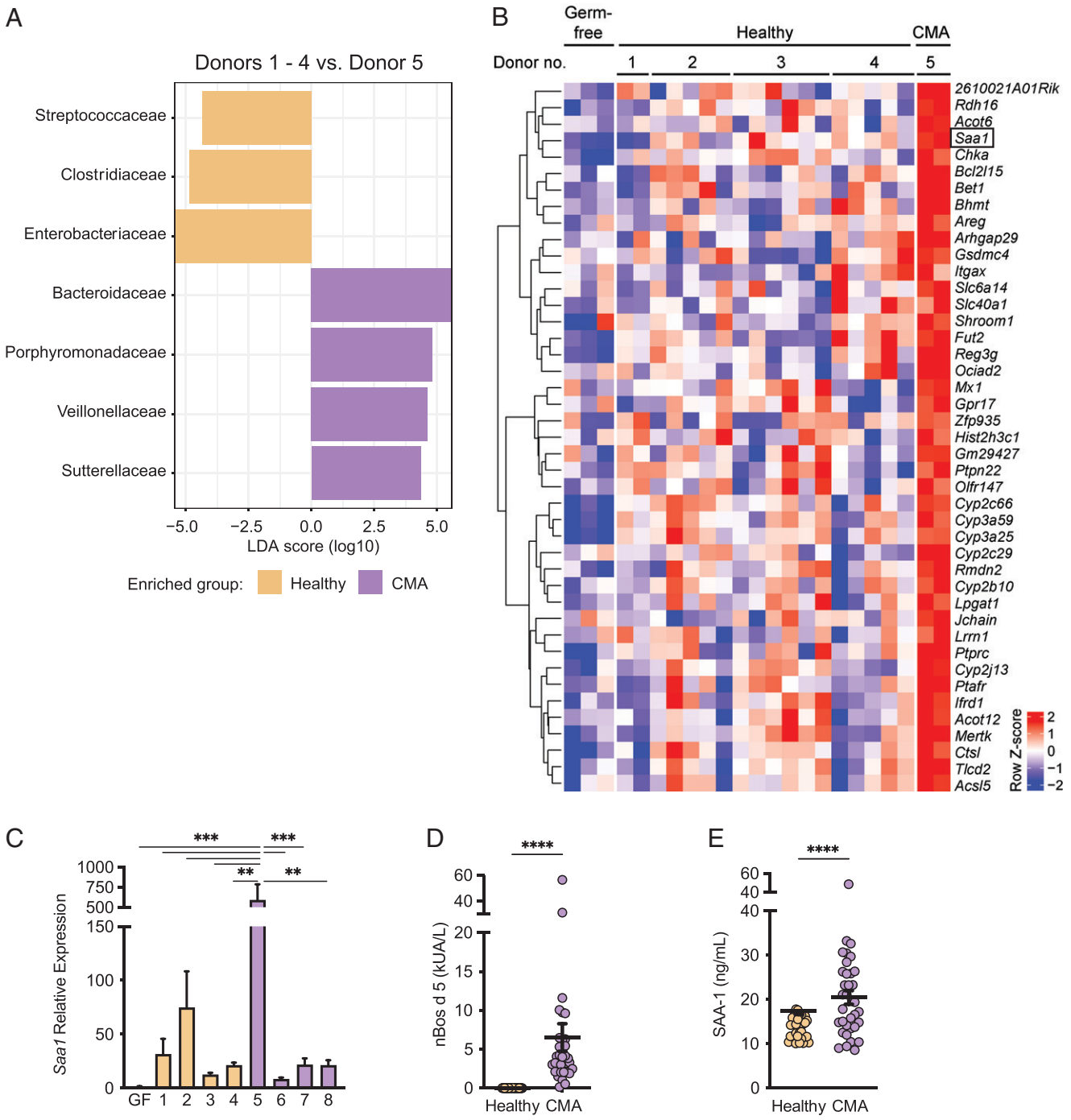

FIGURE 1. The microbiota from a CMA donor is associated with an intestinal inflammatory response. (**A**) Linear discriminant analysis (LDA) effect size showing differentially abundant taxa at the family level in fecal samples between healthy donors 1–4 and CMA donor 5. (**B**) Heatmap of relative abundance of gene transcripts from ileal IECs significantly upregulated in CMA donor 5–colonized mice compared with GF and mice colonized with healthy donors 1–4. (**C**) qRT-PCR analysis of *Saa1* relative expression in GF mice and mice colonized with the microbiota from healthy donors (1–4) and CMA donors (5–8). (**D**) Serum concentrations of IgE specific for the nBos d 5 epitope of BLG and (**E**) SAA-1 from age- and sex-matched pediatric healthy and CMA patients. Symbols represent individual patients, and bars represent mean ± SEM; $n = 30$ patients per group. For (B), significance was determined through Benjamini–Hochberg multiple testing correction, with a FDR ≤ 0.1. For (C), a two-way ANOVA with multiple testing using the Benjamini, Krieger, and Yekutieli method was performed. For (D) and (E), a Wilcoxon rank sum test was performed between both conditions. $^{**}p < 0.01$, $^{***}p < 0.001$, $^{****}p < 0.0001$.

suggest that TLR4 also regulates downstream immune cell populations, including Foxp3$^+$ Tregs and Th17 cells. In the intestinal LP some peripherally induced Foxp3$^+$ Tregs also express the transcription factor RORγt and are reported to be important for the suppression of type 2 inflammation in several mouse models (42, 43). We therefore examined the proportion and absolute numbers of CD4$^+$ Foxp3$^+$ Tregs (referred to as Foxp3$^+$ Tregs) and CD4$^+$Foxp3$^+$ RORγt$^+$ Tregs (referred to as RORγt$^+$ Tregs) in the ileal LP of mice colonized with the CMA or healthy microbiota. GF C57BL/6 TLR4-sufficient and TLR4-deficient mice were colonized with the CMA or healthy microbiota at weaning and euthanized 1 wk later to isolate lymphocytes from the ileal LP. Using the gating strategy shown in Supplemental Fig. 2, flow cytometric analysis revealed that, in TLR4-sufficient but not TLR4-deficient mice, both the

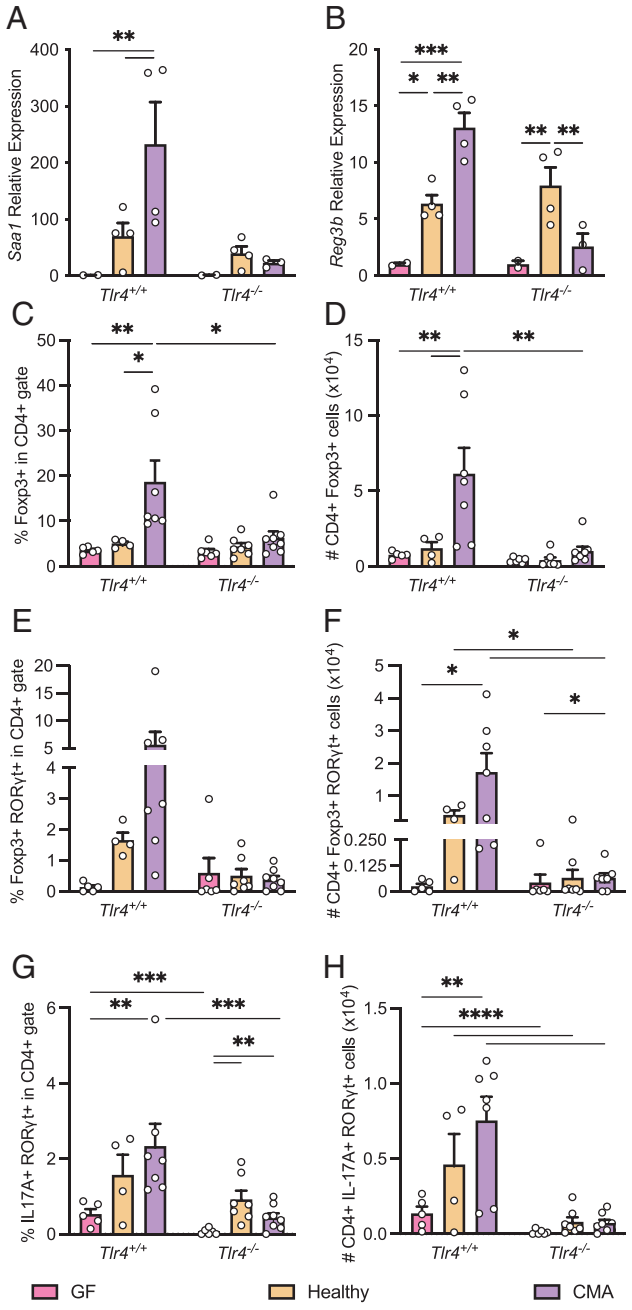

FIGURE 2. TLR4 regulates SAA expression, Tregs, and Th17 cells in the ileum of CMA donor 5–colonized mice. (**A** and **B**) Relative expression of (A) *Saa1* and (B) *Reg3b* in ileal ECs from GF-, healthy-, or CMA-colonized C57BL/6 $Tlr4^{+/+}$ and $Tlr4^{-/-}$ mice at 1 wk postcolonization. (**C**–**H**) Proportion and absolute numbers of (C and D) $CD4^+Foxp3^+$ Tregs, (E and F) $CD4^+Foxp3^+ROR\gamma t^+$ Tregs, and (G and H) $CD4^+IL\text{-}17^+ROR\gamma t^+$ Th17 cells in the ileal LP of $Tlr4^{+/+}$ and $Tlr4^{-/-}$ GF-, healthy-, and CMA-colonized mice. Data are pooled from at least two independent experiments per condition. Statistics were calculated using a two-way ANOVA with multiple testing using the Benjamini, Krieger, and Yekutieli method. $*p < 0.05$, $**p < 0.01$, $***p < 0.001$, $****p < 0.0001$.

proportion and numbers of $Foxp3^+$ Tregs were significantly increased in CMA-colonized mice compared with healthy-colonized mice and GF mice (Fig. 2C, 2D). There was an increased proportion of $ROR\gamma t^+$ Tregs in CMA-colonized mice compared with healthy-colonized and GF mice when TLR4 signaling was sufficient (Fig. 2E) and a decrease in the proportion of this population in TLR4-deficient mice colonized with the CMA microbiota compared with TLR4-sufficient mice. The absolute number of $ROR\gamma t^+$ Tregs was significantly higher in TLR4-sufficient, CMA-colonized mice compared with GF mice of the same genotype (Fig. 2F). There was also a significant reduction in the absolute number of $ROR\gamma t^+$ Tregs in TLR4-deficient, CMA-colonized mice compared with their WT counterparts. This population was significantly reduced in healthy-colonized mice. When we examined Th17 cell populations we found that both the proportion and number of Th17 cells were significantly increased in TLR4-sufficient, CMA-colonized mice compared with GF mice (Fig. 2G, 2H). Importantly, the proportions and numbers of Th17 cells were significantly decreased in TLR4-deficient mice colonized with the CMA-associated microbiota compared with their TLR4-sufficient counterparts. Furthermore, there was a significantly higher proportion of Th17 cells in TLR4-deficient healthy-colonized and CMA-colonized mice compared with GF mice. The absolute number of Th17 cells was also significantly reduced in TLR4-deficient GF and healthy-colonized mice compared with their WT counterparts. Overall, these data show that TLR4 regulates the induction of Tregs and Th17 cells in mice colonized with a CMA microbiota.

TLR4 signaling in the CD11c compartment regulates the expression of alarmins, as well as genes associated with Th17 and B cell responses, in the ileal epithelium of CMA-colonized mice

$CD11c^+$ APCs sample Ags from the intestinal lumen to direct adaptive immunity (44). We next examined the role of TLR4 signaling in $CD11c^+$ APCs in inducing *Saa1* and *Reg3b*, as well as induction of Tregs and Th17 cells. To do this, we used mice with a conditional mutation of TLR4 in $CD11c^+$ cells ($Cd11c^{cre}$ $Tlr4^{fl/fl}$). Because these mice were housed under SPF conditions, we first depleted their microbiota by treating pups with a mixture of antibiotics (see *Materials and Methods*) by intragastric gavage for 7 d prior to weaning. At weaning, these pups were colonized with a CMA or healthy microbiota or left uncolonized as SPF controls. Mice were then euthanized 1 wk later to examine gene expression in ileal IECs. All experiments were littermate controlled. In mice with a conditional mutation of TLR4 in $CD11c^+$ cells, we observed changes in ileal epithelial gene expression similar to those seen in global TLR4 knockout mice. Both *Saa1* and *Reg3b* were significantly upregulated in the ileal epithelium of CMA-colonized $CD11c^{WT}$ mice compared with healthy-colonized mice and SPF controls (Fig. 3A, 3B). However, in their $CD11c^{\Delta TLR4}$ littermates, this upregulation was no longer observed. Because $CD11c^+$ cells have been shown to regulate intestinal IgA through SAA-1 (45), we also examined the expression of the H chain of IgA (*Igha*) and *Jchain*. We observed that *Igha* and *Jchain* were both significantly upregulated in the ileal epithelium of CMA-colonized, $CD11c^{WT}$ mice but not in their $CD11c^{\Delta TLR4}$ littermates (Fig. 3C, 3D, note that our method for isolation of IECs does not include removal of Peyer's patches). These observations correlated with a significant reduction in fecal IgA in $CD11c^{\Delta TLR4}$ mice compared with $CD11c^{WT}$ mice colonized with the CMA microbiota (Fig. 3E).

Alarmins play an important role in initiating type 2 inflammation (46). We used qRT-PCR to examine the expression of the classical epithelial alarmins *Il33*, *Il25*, and *Tslp* in healthy and CMA-colonized $CD11c^{WT}$ and $CD11c^{\Delta TLR4}$ mice. In $CD11c^{WT}$ mice, *Il33* was nearly significantly upregulated ($p = 0.0564$) in CMA-colonized mice compared with both healthy-colonized or SPF mice, which was not seen in $CD11c^{\Delta TLR4}$ littermates (Supplemental Fig. 3A). Conversely, *Il25* was not upregulated in CMA-colonized $CD11c^{WT}$ mice (Supplemental Fig. 3B). However, in $CD11c^{\Delta TLR4}$ mice, *Il25* expression was significantly upregulated in the ileal epithelium of CMA-colonized mice compared with both healthy-colonized and SPF controls. The expression of *Tslp* was not elevated in any of the

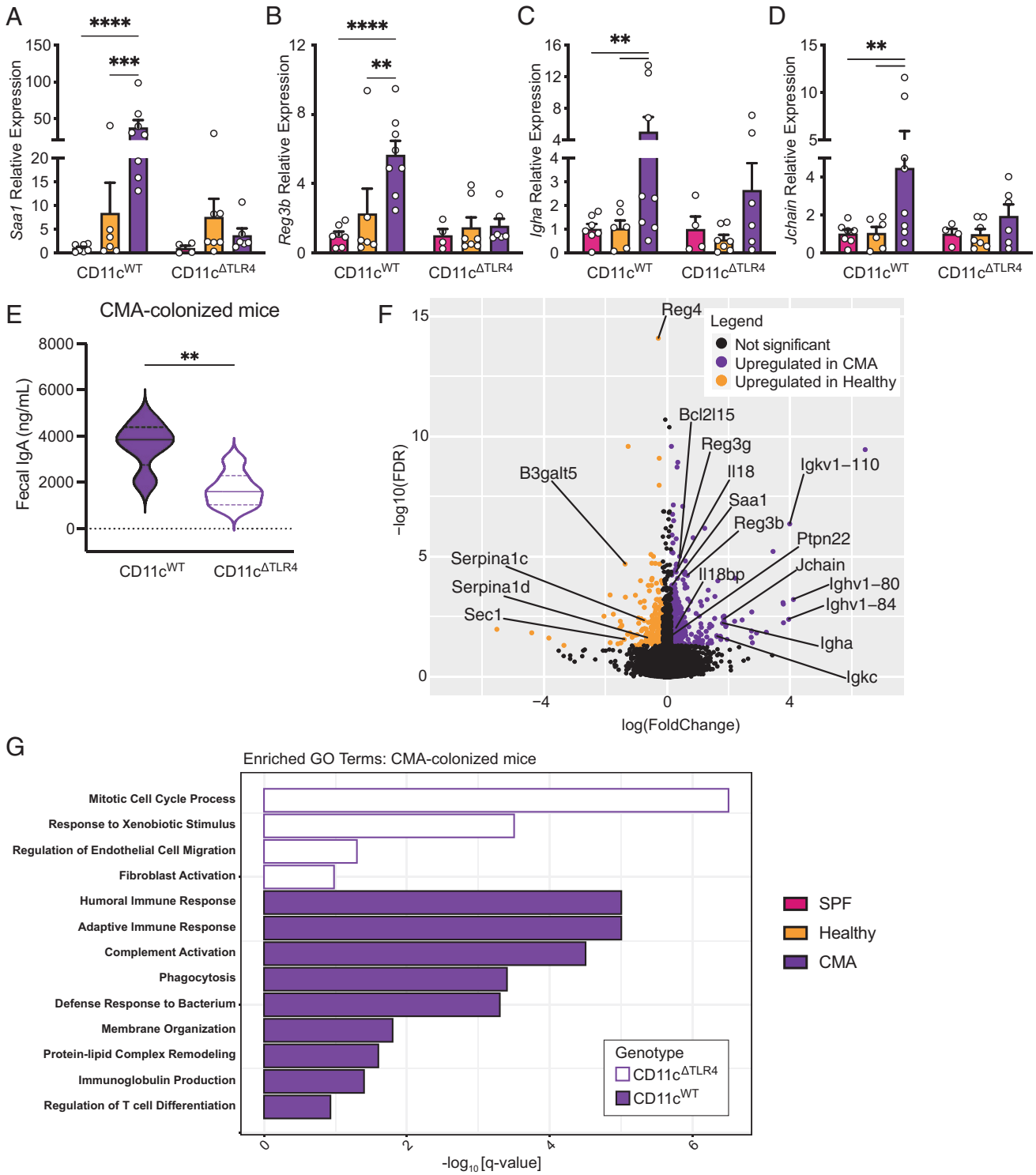

FIGURE 3. TLR4 signaling in the CD11c compartment regulates the expression of genes associated with Th17 and B cell responses in the ileal epithelium of CMA-colonized mice. (**A**–**D**) Relative expression of (A) *Saa1*, (B) *Reg3b*, (C) *Igha*, and (D) *Jchain* in antibiotic-treated SPF mice colonized with a healthy or CMA microbiota or left uncolonized after treatment at 1 wk postcolonization/weaning. (**E**) Fecal IgA levels in antibiotic-treated, CMA-colonized C57BL/6 CD11c^{WT} and CD11c$^{\Delta Tlr4}$ littermates. (**F**) Volcano plot of significantly upregulated genes in antibiotic-treated SPF mice colonized with the CMA or healthy microbiotas. (**G**) Identified Gene Ontology (GO) pathways significantly enriched in ileal IECs of CMA-colonized CD11c^{WT} and CD11c $^{\Delta Tlr4}$ mice. Data are pooled from at least two independent experiments per condition. Statistics were calculated using a two-way ANOVA with multiple testing using the Benjamini, Krieger, and Yekutieli method. $^{**}p < 0.01$, $^{***}p < 0.001$, $^{****}p < 0.0001$.

mice examined (data not shown). These results suggest that TLR4 signaling in the CD11c^{+} compartment regulates type 3 responses, type 2 responses, and B cell responses in the ileum of CMA-colonized mice.

To better understand how TLR4 signaling in CD11c^{+} cells regulates gene expression in the ileal epithelium of CMA-colonized mice, bulk RNA sequencing was conducted on RNA isolated from ileal IECs of antibiotic-treated CD11c^{WT} and CD11c$^{\Delta TLR4}$ mice that

were uncolonized SPF controls, colonized with the CMA microbiota, or colonized with the healthy microbiota. Differential expression analysis between $CD11c^{WT}$ mice colonized with the CMA microbiota and the healthy microbiota revealed several genes to be specifically upregulated in each group. Some of these genes were also upregulated in our previous RNA sequencing dataset (Fig. 1B). Specifically, the expression of *Saa1* was increased, along with other previously identified Th17-associated genes, such as *Reg3b* and *Reg3g* (Fig. 3F). Other genes involved in epithelial-induced proinflammatory responses and barrier function such as *Il18* and *Il18bp* were also upregulated. Many genes related to B cell responses were upregulated, including *Igha*, *Jchain*, and numerous Ig genes. When pathway analysis was conducted on $CD11c^{WT}$ and $CD11c^{\Delta TLR4}$ mice colonized with the CMA microbiota, the results showed that many genes upregulated in $CD11c^{WT}$ mice were involved in immunological processes. In agreement with the differential expression analysis and qRT-PCR data, genes involved in humoral immune responses and Ig production were highly significantly upregulated (Fig. 3G). Genes involved in regulation of T cell differentiation were also significantly upregulated, in agreement with our previous data showing that global TLR4 signaling regulates several T cell subsets in CMA-colonized mice (Fig. 2C–H). Interestingly, genes involved in defense against bacteria were also upregulated in $CD11c^{WT}$, but not $CD11c^{\Delta TLR4}$, mice. The pathways upregulated in $CD11c^{\Delta TLR4}$ mice were more aligned with homeostatic regulation of the epithelium.

To better understand the bacterial communities that induce these genes in CMA- and healthy-colonized mice, 16S sequencing was performed on samples of ileal contents acquired from these mice at euthanasia. Because these mice originated from a SPF colony and were treated with antibiotics, the gut microbiota will consist of an amalgamation of bacteria originating from the SPF microbiota and human-derived bacteria from the infant donors. Therefore, we first performed a basic, holistic analysis of α and β diversity to assess the ecological dynamics of the commensal microbiota and determine the fidelity of transfer of the human infant microbiota. The Shannon index was used to calculate diversity within each sample. Analysis of each sample by group determined that the average diversity within each sample did not significantly differ with colonization status (Supplemental Fig. 3C). To determine the fidelity of transfer, β diversity was determined using the Bray–Curtis index of dissimilarity. Analysis between groups showed that there were significant differences between microbial communities based on colonization status (Supplemental Fig. 3D). This suggests that the transfer of the human infant gut microbiota following antibiotic treatment of SPF mice was successful and that differences in gene expression observed in CMA- and healthy-colonized mice were due to the infant microbiotas. In summary, these data show that in our antibiotic-treated SPF model, the phenotypic upregulation of *Saa1* and *Reg3b* (as well as numerous other immune system genes) in isolated ileal IECs and the production of fecal IgA are most likely due to the engraftment of the CMA microbiota.

Th17 and B cell–associated genes are regulated by TLR4 signaling in $CD11c^+$ cells in GF mice colonized with the CMA microbiota

We have shown that global expression of TLR4 and its conditional expression in $CD11c^+$ cells regulates ileal IEC gene expression in CMA-colonized mice in both GF and antibiotic-treated colonization models, respectively. To gain insight into the taxa in the CMA donor 5 microbiota that may contribute to these immune responses, we rederived SPF $CD11c^{WT}$ and $CD11c^{\Delta TLR4}$ mice as GF. The experiments that were performed in the antibiotic-treated model were repeated using these GF mice following the same experimental protocol used in the global TLR4-deficient mice. The mice were colonized at weaning with the CMA or healthy microbiota and euthanized at 1 wk postcolonization to isolate RNA from ileal IECs and examine *Saa1* expression. Expression analysis showed results that were strikingly similar to those observed in global and CD11c-conditional TLR4-deficient mice. *Saa1* and *Reg3b* were significantly upregulated in $CD11c^{WT}$ CMA-colonized mice compared with healthy-colonized and GF mice (Fig. 4A, 4B). However, in CMA-colonized mice with a conditional mutation in TLR4 in $CD11c^+$ cells, these genes were no longer upregulated. We also observed that the expression of the B cell–related genes *Igha* and *Jchain* were significantly increased in CMA-colonized mice compared with GF mice and were regulated by TLR4 signaling in $CD11c^+$ cells (Fig. 4C, 4D). This translated to differences in the production of fecal IgA. In $CD11c^{WT}$ mice, fecal IgA was significantly higher in CMA-colonized mice compared with healthy-colonized and GF mice (Fig. 4E). In $CD11c^{\Delta TLR4}$ mice, there was significantly higher fecal IgA in CMA-colonized and healthy-colonized mice compared with GF mice. Interestingly, there was a significant reduction in fecal IgA in CMA-colonized $CD11c^{\Delta TLR4}$ mice compared with their $CD11c^{WT}$ littermates. This significant reduction was not observed between $CD11c^{WT}$ and $CD11c^{TLR4}$ mice colonized with the healthy microbiota or $CD11c^{WT}$ and $CD11c^{\Delta TLR4}$ GF mice. These data therefore show that TLR4 signaling in $CD11c^+$ cells regulates the expression of *Saa1* and *Reg3b* in ileal IECs of CMA-colonized mice in both the GF and antibiotic-treated colonization models. Furthermore, in CMA-colonized mice, TLR4 signaling in $CD11c^+$ cells regulates B cell responses and intestinal IgA production.

TLR4 signaling in $CD11c^+$ cells regulates Th17 but not Treg populations in the ileum of CMA-colonized mice

Because similar gene expression results were seen in GF mice with a global deficiency in TLR4, we examined whether TLR4 signaling in $CD11c^+$ cells also regulated T cell populations. We observed that TLR4 signaling in $CD11c^+$ cells did not regulate T cell populations in the same way that global TLR4 signaling did. Both CMA- and healthy-colonized mice had significantly greater proportions of $Foxp3^+$ Tregs compared with GF mice when TLR4 signaling was sufficient in $CD11c^+$ cells (Fig. 4F). The absolute number of $Foxp3^+$ Tregs was also significantly higher in $CD11c^{WT}$, CMA-colonized mice compared with their GF counterparts (Fig. 4G). The proportion of $ROR\gamma t^+$ Tregs was increased in $CD11c^{WT}$ mice colonized with the CMA microbiota compared with GF mice (Fig. 4H). However, the proportion and absolute number of both $Foxp3^+$ Tregs and $Foxp3^+ROR\gamma t^+$ Tregs was not different between $CD11c^{WT}$ and $CD11c^{\Delta TLR4}$ littermates in all colonization conditions (Fig. 4F–I). This suggests that TLR4 signaling in another cellular compartment modulates the Treg populations that are induced by the CMA microbiota. When we examined Th17 populations, we observed that in $CD11c^{WT}$ mice, there were significantly higher proportions in healthy and CMA-colonized mice compared with GF mice (Fig. 4J). Furthermore, the frequency of this population was significantly reduced in $CD11c^{\Delta TLR4}$ mice colonized with the CMA microbiota compared with their WT littermates. This reduction was also observed in the absolute numbers of Th17 cells (Fig. 4K). The absolute number of Th17 cells in CMA-colonized mice was also greater compared with healthy-colonized and GF mice when TLR4 signaling was sufficient in $CD11c^+$ cells. In $CD11c^{\Delta TLR4}$ mice, the proportion and absolute number of Th17 cells was significantly higher in CMA-colonized mice compared with GF mice (Fig. 4K). Representative dot plots for $Foxp3^+ROR\gamma t^+$ Treg populations and $IL\text{-}17A^+ROR\gamma t^+$ Th17 cells in GF, healthy, or CMA-colonized $CD11c^{WT}$ mice are shown in Fig. 4L. These results show that in CMA-colonized mice, TLR4 signaling in $CD11c^+$ cells regulates Th17 but not Treg populations. This agrees with previous findings that SAA-1 induces Th17 differentiation only in the presence of $CD11c^+$ dendritic cells (DCs) from

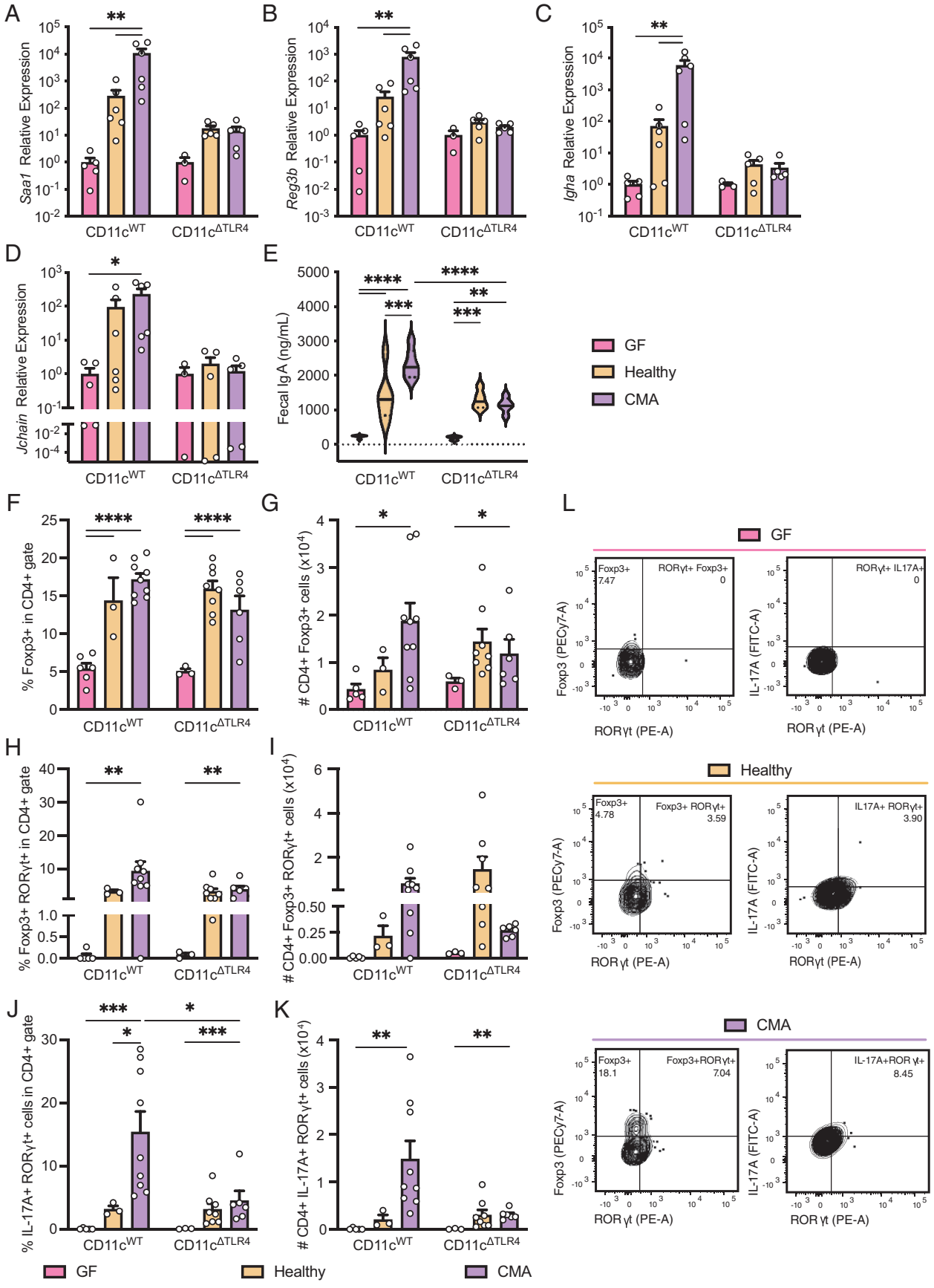

FIGURE 4. Th17- and B cell–associated genes are regulated by TLR4 signaling in CD11c$^+$ cells in GF mice colonized with the CMA microbiota. (**A**–**D**) Relative expression of (A) *Saa1*, (B) *Reg3b*, (C) *Igha*, and (D) *Jchain* in GF-, healthy-, and CMA-colonized mice at 1 wk postcolonization. (**E**) Fecal IgA levels of GF-, healthy-, and CMA-colonized CD11c^{WT} and CD11c$^{\Delta Tlr4}$ mice. (**F**–**K**) Proportion and absolute numbers of (F and G) CD4$^+$Foxp3$^+$Tregs, (H and I) CD4$^+$Foxp3$^+$RORγt$^+$ Tregs, and (J and K) CD4$^+$IL-17$^+$RORγt$^+$ Th17 cells in the ileal LP of GF-, healthy-, and *(Figure legend continues)*

the LP (47). Taken together, these data show that while global TLR4 signaling regulates the induction of Tregs and Th17 cells in CMA-colonized mice, TLR4 signaling in CD11c$^+$ cells specifically regulates the induction of Th17 cells.

Elevation of IL-17 and IL-13 in BLG-sensitized, CMA-colonized mice is dependent on TLR4 in CD11c$^+$ cells

We have shown that this CMA microbiota induces transient inflammation characterized by the induction of IgA, antimicrobial peptides, and Th17 cells and that these responses are regulated by TLR4 signaling in CD11c$^+$ cells. To examine the role of TLR4 signaling in regulating Th2-mediated allergic inflammation, CD11c$^{\Delta TLR4}$ and CD11c^{WT} littermates were colonized with the CMA or healthy microbiota and sensitized with BLG plus CT, and splenocytes were restimulated with Ag in vitro, as outlined in *Materials and Methods*. Supernatants of these cultures were examined for IL-13 (Th2) and IL-17 (Th17) production cytokines (48). BLG-stimulated splenocytes produced significantly higher levels of IL-17 and IL-13 compared with the unstimulated condition in CMA-colonized, CD11c^{WT} mice, but not their CD11c$^{\Delta TLR4}$ littermates (Supplemental Fig. 3E, 3F). Stimulation with BLG did not result in elevated IL-13 and IL-17 levels in healthy-colonized mice compared with unstimulated splenocytes, regardless of genotype. TLR4-sufficient CMA-colonized mice produced elevated levels ($p = 0.0651$) of IL-13 (Supplemental Fig. 3E) and significantly higher levels of IL-17 (Supplemental Fig. 3F) compared with their CD11c$^{\Delta TLR4}$ counterparts. This difference was not observed in healthy-colonized mice, as both CD11c^{WT} and CD11c$^{\Delta TLR4}$ produced comparable levels of IL-17 and IL-13. This is in alignment with our previous data showing that TLR4 signaling in CD11c$^+$ cells specifically regulates Th17 populations in the ileum of CMA-colonized mice and expands this finding to an atopic context. We also analyzed production of intestinal cytokines from these sensitized mice by quantifying transcripts of *Il13* and *Il17a* by qRT-PCR in the ileal LP. CMA-colonized CD11c^{WT} mice had significantly higher *Il17a* transcripts compared with both healthy-colonized CD11c^{WT} mice and CMA-colonized CD11c$^{\Delta TLR4}$ counterparts (Supplemental Fig. 3H). *Il13* was similarly elevated in CMA-colonized CD11c^{WT} and CD11c$^{\Delta TLR4}$ mice, although differences were not significant (Supplemental Fig. 3G).

CMA-colonized mice have higher representation of Gram-negative bacteria in their ileal contents

Rederivation of GF mice with a conditional mutation of TLR4 in CD11c$^+$ cells allowed us to examine microbes that may contribute to *Saa1* expression, an analysis that was not possible in the antibiotic treatment model. To determine microbial contributors to the observed TLR4-dependent phenotypes, we conducted 16S rRNA sequencing on ileal samples of CMA- and healthy-colonized CD11c^{WT} and CD11c$^{\Delta TLR4}$ mice. We found that multiple taxa were differentially abundant between healthy and CMA-colonized mice. In healthy-colonized mice several clostridial taxa were significantly more abundant, including Lachnospiraceae and *Clostridium* cluster XIVa, which we have previously reported to be barrier protective Clostridia (11, 12) (Supplemental Fig. 4A). Importantly, all Gram-negative bacteria that were identified as differentially abundant were significantly higher in CMA-colonized mice compared with healthy-colonized mice (Supplemental Fig. 4B). After obtaining these results, we followed up with shotgun metagenomic sequencing of the same samples (CD11c^{WT} and CD11cΔ^{TLR4}) to get a more resolved understanding of which species were differentially abundant between healthy- and CMA-colonized mice. Metagenomic analysis showed that the bacterial communities in the healthy- and CMA-colonized mice were markedly different (Fig. 5A). In agreement with the 16S data, CMA-colonized mice had an expansion of Gram-negative bacteria, such as Proteobacteria and Bacteroidetes. Healthy-colonized mice had a higher abundance of *Enterococcus* and Lachnospiraceae, which was also in agreement with the 16S data. No significant differences were noted for the CD11c^{WT} and CD11cΔ^{TLR4} genotypes of the healthy- and CMA-colonized mice. We therefore pooled these genotypes for further analysis of the healthy and CMA microbiomes. As expected, the ileal bacterial communities of healthy-colonized and CMA-colonized mice were distinct according to β diversity metrics (Fig. 5B). Differential abundance analysis of shotgun metagenomic sequences revealed numerous bacterial species to be significantly enriched in healthy- or CMA-colonized mice. Interestingly, we saw that, in agreement with the 16S sequencing data, Gram-negative species were significantly more abundant in CMA-colonized mice than in healthy-colonized mice (Fig. 5C). These Gram-negative species included multiple taxa in the phyla Bacteroidetes, Protobacteria (*Enterobacter hormaechei*, *Escherichia coli*), and Verrucomicrobiota (*Akkermansia muciniphila*, Fig. 5C). Other differentially abundant taxa are shown in Supplemental Fig. 5. When we analyzed the representation of LPS synthesis and LPS modification genes in these samples, we saw that all genes analyzed had significantly greater representation in CMA-colonized mice, except for lpxE, which was significantly higher in healthy-colonized mice (Fig. 5D). Taken together, these data show that the CMA microbiota has higher abundance of Gram-negative bacteria and increased representation of LPS genes.

Discussion

In the context of FAs and other atopic diseases, the epithelium acts not only as a barrier between exogenous Ags and the immune system, but it also receives signals from these Ags through innate receptors and relays information about them to local immune cells. This surveillance feature of the epithelium is important for mounting appropriate immune responses to allergens and noxious substances (3). In the data presented in the current study, we employed multiple colonization models to show that the microbiota of a particular CMA infant (donor 5) induces a mixed inflammatory response in the ileal epithelium. This not only includes the induction of *Saa1* and *Reg3b*, but other inflammatory and mucosal genes such as *Il33*, *Il13ra, Il15*, and *Il18*. In the clinic, SAA-1 has been used as a biomarker of systemic inflammation for patients with Crohn's disease as well as patients with allergic asthma (49–51). More recently, it has been shown to be induced in the intestinal and bronchial epithelium and can regulate type 2 and type 3 inflammation at those sites (41, 48). Furthermore, *Saa1* can be induced in the terminal ileal epithelium by segmented filamentous bacteria, *Citrobacter rodentium*, *E. coli* O157, and other epithelial-adherent bacteria (37). The changes in epithelial gene expression induced in response to colonization with the CMA donor 5 microbiota suggested that this may be a proinflammatory bacterial community distinct from that of the healthy infant donors.

CMA-colonized CD11c^{WT} and CD11c$^{\Delta Tlr4}$ mice at 1 wk postcolonization/weaning. (**L**) Representative plots of Treg (both CD4$^+$Foxp3$^+$ and CD4$^+$Foxp3$^+$ RORγt$^+$ Treg populations, left plot) and CD4$^+$IL-17$^+$RORγt$^+$ cell populations (right plot). Plots from one representative CD11c^{WT} mouse are shown for each condition (GF, healthy, and CMA). Data are pooled from at least two independent experiments per condition. Statistics were calculated using a two-way ANOVA with multiple testing using the Benjamini, Krieger, and Yekutieli method. *$p < 0.05$, **$p < 0.01$, ***$p < 0.001$, ****$p < 0.0001$.

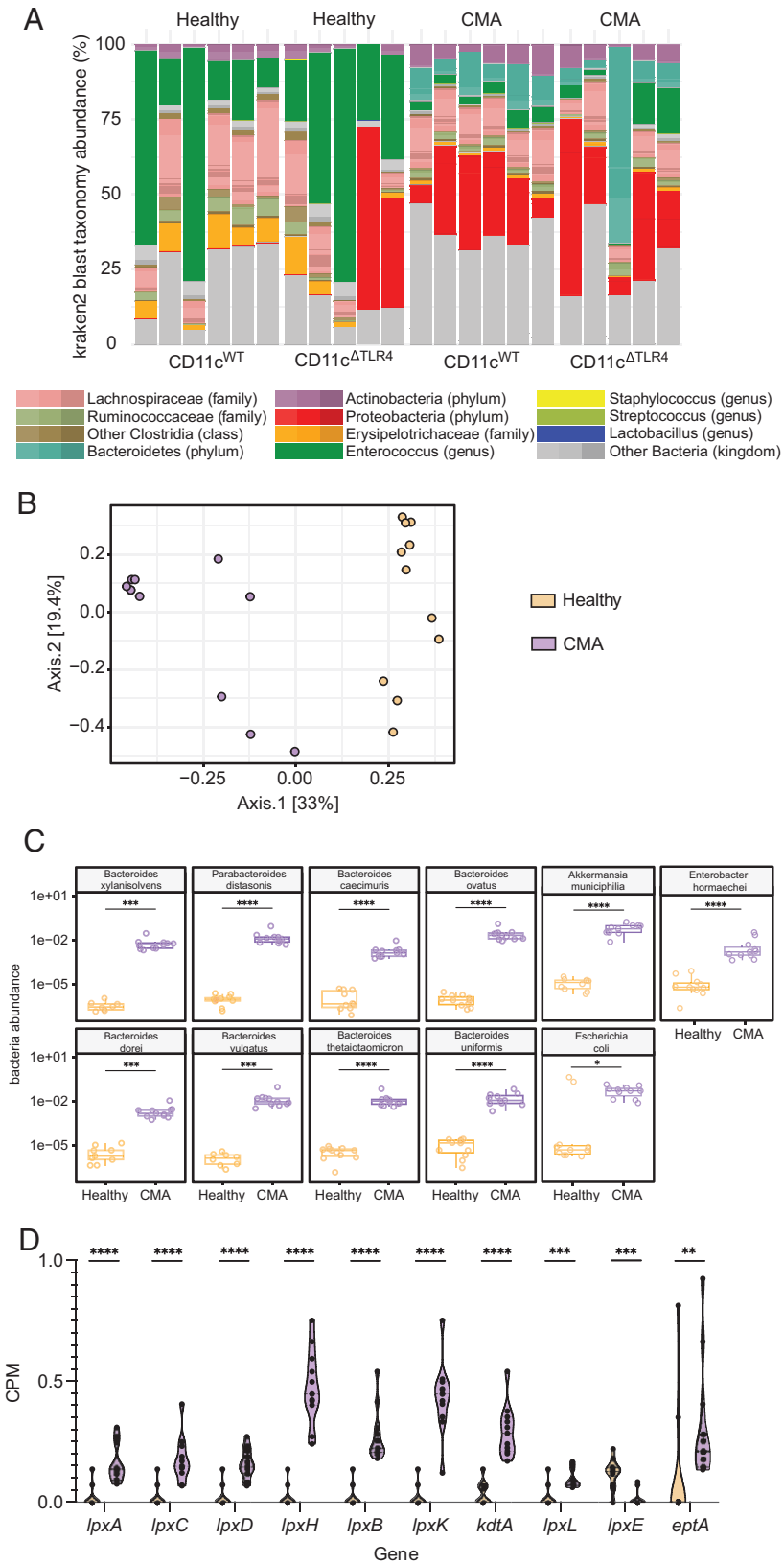

FIGURE 5. CMA-colonized mice harbor an increased abundance of Bacteroidetes and other Gram-negative bacteria in ileal contents. (**A**) Relative abundance of metagenomic reads as classified by Kraken2 in ileal contents of healthy- and CMA-colonized mice with and without a conditional mutation of TLR4 in CD11c^{+} cells at 1 wk postcolonization. (**B**) β Diversity of healthy and CMA-colonized mice using the Bray–Curtis metric. (**C**) Differentially abundant Gram-negative species between healthy and CMA-colonized mice. (**D**) Counts per million of genes involved in KEGG pathways related to KDO2–lipid A biosynthesis and modification. WT and TLR4 mutant genotypes in (A) were pooled for the analyses in (B)–(D). Statistics were calculated by performing a Wilcoxon rank sum test between both conditions. $^{**}p < 0.01$, $^{***}p < 0.001$, $^{****}p < 0.0001$.

Gram-negative bacteria, particularly Bacteroidales (Bacteroidaceae and Porphyromonadaceae) and Proteobacteria were enriched in the CMA donor 5 microbiota compared with all healthy infant donors. An earlier study found that Bacteroidetes was enriched in two cohorts of infants with increased prevalence of allergy and autoimmunity compared with a genetically similar cohort with decreased prevalence of these diseases (52). Moreover, this study showed that LPS from several Bacteroidetes species was hypoimmunogenic and not protective against the onset of diabetes in a mouse model, unlike LPS from *E. coli* (Proteobacteria), which was hyperimmunogenic and protective. Interestingly, more recent work shows that myeloid cells can distinguish the Gram-negative taxa Bacteroidetes and Proteobacteria by differential signaling through TLR2 and TLR4, respectively (53). SAA-1 has been shown to bind to LPS, opsonize Gram-negative bacteria, and mediate their phagocytosis (39, 54). Furthermore, SAA-1 can induce inflammatory cytokine expression in macrophages in a TLR4-dependent manner (54). We found that the microbiota from CMA donor 5 (but not other CMA donors) induces upregulation of *Saa1* in the ileal epithelium and demonstrated that serum SAA-1 may have the potential to be a biomarker of allergic inflammation in a subset of patients with FA. Downstream of this initial inflammatory *Saa1* response, Treg and Th17 cell populations were significantly induced, along with fecal IgA, in CMA-colonized mice in comparison with healthy-colonized mice. The atopic symptoms that CMA donor 5 exhibited within minutes after feeding (i.e., vomiting, urticaria), as well as the gastrointestinal inflammation (nodular hyperplasia and eosinophilic infiltration) were likely the outcome of a vigorous allergen-specific response that developed within the first months of the infant's life. In this study, we examined an early snapshot of the inflammatory response associated with this microbiota.

In addition to the inflammatory transcriptional profile induced in the ileal mucosa, significantly elevated proportions, and numbers of $Foxp3^+$ Tregs, $Foxp3^+ROR\gamma t^+$ Tregs, and $IL\text{-}17A^+ROR\gamma t^+$ Th17 cells, as well as increased induction of IgA, were specific to mice colonized with the CMA microbiota and were regulated by TLR4 signaling. It has been well documented that TLR4 signaling in various cellular compartments differentially regulates allergic inflammation (55, 56). $CD11c^+$ DCs that are activated by SAA-1 promote IL-17A production in $CD4^+$ T cells, contributing to Th2 and Th17 inflammatory responses in a model of allergic asthma (57). Furthermore, DCs have been specifically shown to regulate T and B cell responses through binding of retinol/SAA-1 complexes in the intestine (45). *Saa1* is induced in the ileal epithelium by epithelial-adherent bacteria and is downstream of the IL-23 signaling axis initiated by intestinal DCs in response to microbial stimulation (58). Induction of *Saa1* by the epithelium increases the production of IgA by B cells and IL-17A in Th17 cells and leads to the exacerbation of intestinal inflammation caused by this T cell subset (37, 41). In agreement with previous reports, our data show that the induction of effector Th17 cells and IgA production by the CMA microbiota was coregulated with the induction of *Saa1* and dependent on TLR4 signaling in $CD11c^+$ cells. Interestingly, Tregs were also highly induced in CMA-colonized mice. This is in alignment with previous studies observing robust induction of $Foxp3^+$ Tregs and $Foxp3^+ROR\gamma t^+$ Tregs in response to gut inflammation induced by Gram-negative bacteria, which required TLR4 signaling (59, 60). Our observation that the induction of Tregs is independent of TLR4 signaling in $CD11c^+$ cells also agrees with previous reports showing that induction of *Saa1* induces Th17 cells and intestinal IgA but not Tregs (45, 47). With the production of SAA-1 favoring induction of Th17 cells, coupled with type 2 and type 3 inflammatory signals from the epithelium, the increased induction of Tregs may be a compensatory mechanism to address inflammation within the local microenvironment.

Rederivation of $CD11c^{cre}TLR4^{fl/fl}$ mice as GF allowed us to identify bacteria enriched in CMA-colonized mice without contamination from the SPF commensal microbiota. Through use of this gnotobiotic model we were able to determine that Gram-negative bacteria, particularly Bacteroidetes and Proteobacteria, are specifically enriched in the CMA microbiota. The Bacteroidetes species are known to be common commensals of the mammalian intestine (61). Although some have been documented to promote intestinal health (62), others have been associated with intestinal inflammation, and, particularly, the induction of *Saa1* in the ileal epithelium (37, 63). Moreover, increased SAA-1 expression and Th17 cells have been correlated with increased abundance of *Bacteroides* in ileal biopsies from inflammatory bowel disease patients (40). As *Saa1* has been shown to contribute to allergic inflammation (48), it is reasonable to suspect that induction of *Saa1* by a Bacteroidetes-enriched microbiota contributes to FAs. Very few studies have examined an intestinal inflammatory response in the context of an IgE-mediated FA. This study is (to our knowledge) novel in its association of a microbiota rich in Gram-negative bacteria with the induction of type 2/type 3 inflammation prior to and following sensitization with the cow's milk allergen BLG. Earlier work showed that enriched biosynthesis of LPS genes was characteristic of allergic children in a large (90 patient) group from the same demographic cohort (16). We selected one patient for a mechanistic examination of how Gram-negative bacteria contribute to the allergic response induced in a gnotobiotic model. The observation that SAA-1 is elevated in the serum of a subset of infants in the larger cohort suggests that the intestinal inflammation that is associated with donor 5 is relevant to other infants with CMA. Because FAs and other atopic diseases elicit diverse immunological responses, the use of SAA-1 as a biomarker may characterize a specific type of inflammatory response in CMA.

Acknowledgments

We thank the staff of the University of Chicago Animal Resource Center, particularly the Gnotobiotic Research Animal Facility, for expert technical assistance. We also thank the Duchossois Family Institute for help with bioinformatics analysis. The visual abstract was generated using BioRender.com.

Disclosures

C.R.N. is a cofounder of ClostraBio, Inc. The other authors have no financial conflicts of interest.

References

1. Gupta, R. S., E. E. Springston, M. R. Warrier, B. Smith, R. Kumar, J. Pongracic, and J. L. Holl. 2011. The prevalence, severity, and distribution of childhood food allergy in the United States. *Pediatrics* 128: e9–e17.
2. Brough, H. A., B. J. Lanser, S. B. Sindher, J. M. C. Teng, D. Y. M. Leung, C. Venter, S. M. Chan, A. F. Santos, H. T. Bahnson, E. Guttman-Yassky, et al. 2022. Early intervention and prevention of allergic diseases. *Allergy* 77: 416–441.
3. Iweala, O. I., and C. R. Nagler. 2019. The microbiome and food allergy. *Annu. Rev. Immunol.* 37: 377–403.
4. Warren, C. M., J. Jiang, and R. S. Gupta. 2020. Epidemiology and burden of food allergy. *Curr. Allergy Asthma Rep.* 20: 6.
5. Renz, H., and C. Skevaki. 2021. Early life microbial exposures and allergy risks: opportunities for prevention. *Nat. Rev. Immunol.* 21: 177–191.
6. Marra, F., C. A. Marra, K. Richardson, L. D. Lynd, A. Kozyrskyj, D. M. Patrick, W. R. Bowie, and J. M. Fitzgerald. 2009. Antibiotic use in children is associated with increased risk of asthma. *Pediatrics* 123: 1003–1010.
7. Russell, S. L., M. J. Gold, M. Hartmann, B. P. Willing, L. Thorson, M. Wlodarska, N. Gill, M. R. Blanchet, W. W. Mohn, K. M. McNagny, and B. B. Finlay. 2012. Early life antibiotic-driven changes in microbiota enhance susceptibility to allergic asthma. *EMBO Rep.* 13: 440–447.
8. Metsälä, J., A. Lundqvist, L. J. Virta, M. Kaila, M. Gissler, and S. M. Virtanen. 2013. Mother's and offspring's use of antibiotics and infant allergy to cow's milk. *Epidemiology* 24: 303–309.
9. Bashir, M. E., S. Louie, H. N. Shi, and C. Nagler-Anderson. 2004. Toll-like receptor 4 signaling by intestinal microbes influences susceptibility to food allergy. *J. Immunol.* 172: 6978–6987.
10. Noval Rivas, M., O. T. Burton, P. Wise, Y. Q. Zhang, S. A. Hobson, M. Garcia Lloret, C. Chehoud, J. Kuczynski, T. DeSantis, J. Warrington, et al. 2013. A

microbiota signature associated with experimental food allergy promotes allergic sensitization and anaphylaxis. *J. Allergy Clin. Immunol.* 131: 201–212.
11. Stefka, A. T., T. Feehley, P. Tripathi, J. Qiu, K. McCoy, S. K. Mazmanian, M. Y. Tjota, G. Y. Seo, S. Cao, B. R. Theriault, et al. 2014. Commensal bacteria protect against food allergen sensitization. *Proc. Natl. Acad. Sci. USA* 111: 13145–13150.
12. Feehley, T., C. H. Plunkett, R. Bao, S. M. Choi Hong, E. Culleen, P. Belda-Ferre, E. Campbell, R. Aitoro, R. Nocerino, L. Paparo, et al. 2019. Healthy infants harbor intestinal bacteria that protect against food allergy. *Nat. Med.* 25: 448–453.
13. Abdel-Gadir, A., E. Stephen-Victor, G. K. Gerber, M. Noval Rivas, S. Wang, H. Harb, L. Wang, N. Li, E. Crestani, S. Spielman, et al. 2019. Microbiota therapy acts via a regulatory T cell MyD88/RORγt pathway to suppress food allergy. [Published erratum appears in 2019 *Nat. Med.* 25: 1458.] *Nat. Med.* 25: 1164–1174.
14. Wang, R., S. Cao, M. E. H. Bashir, L. A. Hesser, Y. Su, S. M. C. Hong, A. Thompson, E. Culleen, M. Sabados, N. P. Dylla, et al. 2023. Treatment of peanut allergy and colitis in mice via the intestinal release of butyrate from polymeric micelles. *Nat. Biomed. Eng.* 7: 38–55.
15. Berni Canani, R., N. Sangwan, A. T. Stefka, R. Nocerino, L. Paparo, R. Aitoro, A. Calignano, A. A. Khan, J. A. Gilbert, and C. R. Nagler. 2016. *Lactobacillus rhamnosus* GG-supplemented formula expands butyrate-producing bacterial strains in food allergic infants. *ISME J.* 10: 742–750.
16. De Filippis, F., L. Paparo, R. Nocerino, G. Della Gatta, L. Carucci, R. Russo, E. Pasolli, D. Ercolini, and R. Berni Canani. 2021. Specific gut microbiome signatures and the associated pro-inflamatory functions are linked to pediatric allergy and acquisition of immune tolerance. *Nat. Commun.* 12: 5958.
17. Nik, A. M., and P. Carlsson. 2013. Separation of intact intestinal epithelium from mesenchyme. *Biotechniques* 55: 42–44.
18. Gracz, A. D., B. J. Puthoff, and S. T. Magness. 2012. Identification, isolation, and culture of intestinal epithelial stem cells from murine intestine. *Methods Mol. Biol.* 879: 89–107.
19. Moro, K., K. N. Ealey, H. Kabata, and S. Koyasu. 2015. Isolation and analysis of group 2 innate lymphoid cells in mice. *Nat. Protoc.* 10: 792–806.
20. Upadhyay, V., V. Poroyko, T. J. Kim, S. Devkota, S. Fu, D. Liu, A. V. Tumanov, E. P. Koroleva, L. Deng, C. Nagler, et al. 2012. Lymphotoxin regulates commensal responses to enable diet-induced obesity. *Nat. Immunol.* 13: 947–953.
21. Salzman, N. H., K. Hung, D. Haribhai, H. Chu, J. Karlsson-Sjöberg, E. Amir, P. Teggatz, M. Barman, M. Hayward, D. Eastwood, et al. 2010. Enteric defensins are essential regulators of intestinal microbial ecology. *Nat. Immunol.* 11: 76–83.
22. Godínez-Victoria, M., R. Campos-Rodriguez, V. Rivera-Aguilar, E. Lara-Padilla, J. Pacheco-Yepez, R. A. Jarillo-Luna, and M. E. Drago-Serrano. 2014. Intermittent fasting promotes bacterial clearance and intestinal IgA production in *Salmonella typhimurium*-infected mice. *Scand. J. Immunol.* 79: 315–324.
23. Cautivo, K. M., P. R. Matatia, C. O. Lizama, N. M. Mroz, M. W. Dahlgren, X. Yu, J. Sbierski-Kind, M. T. Taruselli, J. F. Brooks, A. Wade-Vallance, et al. 2022. Interferon gamma constrains type 2 lymphocyte niche boundaries during mixed inflammation. *Immunity* 55: 254–271.e7.
24. Liao, Y., G. K. Smyth, and W. Shi. 2019. The R package Rsubread is easier, faster, cheaper and better for alignment and quantification of RNA sequencing reads. *Nucleic Acids Res.* 47: e47.
25. Chen, Y., A. T. Lun, and G. K. Smyth. 2016. From reads to genes to pathways: differential expression analysis of RNA-Seq experiments using Rsubread and the edgeR quasi-likelihood pipeline. *F1000 Res.* 5: 1438.
26. Zhou, Y., B. Zhou, L. Pache, M. Chang, A. H. Khodabakhshi, O. Tanaseichuk, C. Benner, and S. K. Chanda. 2019. Metascape provides a biologist-oriented resource for the analysis of systems-level datasets. *Nat. Commun.* 10: 1523.
27. Bolyen, E., J. R. Rideout, M. R. Dillon, N. A. Bokulich, C. C. Abnet, G. A. Al-Ghalith, H. Alexander, E. J. Alm, M. Arumugam, F. Asnicar, et al. 2019. Reproducible, interactive, scalable and extensible microbiome data science using QIIME 2. [Published erratum appears in 2019 *Nat. Biotechnol.* 37: 1091.] *Nat. Biotechnol.* 37: 852–857.
28. Callahan, B. J., P. J. McMurdie, M. J. Rosen, A. W. Han, A. J. Johnson, and S. P. Holmes. 2016. DADA2: high-resolution sample inference from Illumina amplicon data. *Nat. Methods* 13: 581–583.
29. Wang, Q., G. M. Garrity, J. M. Tiedje, and J. R. Cole. 2007. Naive Bayesian classifier for rapid assignment of rRNA sequences into the new bacterial taxonomy. *Appl. Environ. Microbiol.* 73: 5261–5267.
30. Bodenhofer, U., E. Bonatesta, C. Horejš-Kainrath, and S. Hochreiter. 2015. msa: an R package for multiple sequence alignment. *Bioinformatics* 31: 3997–3999.
31. Li, D., C. M. Liu, R. Luo, K. Sadakane, and T. W. Lam. 2015. MEGAHIT: an ultra-fast single-node solution for large and complex metagenomics assembly via succinct de Bruijn graph. *Bioinformatics* 31: 1674–1676.
32. Hyatt, D., G. L. Chen, P. F. Locascio, M. L. Land, F. W. Larimer, and L. J. Hauser. 2010. Prodigal: prokaryotic gene recognition and translation initiation site identification. *BMC Bioinformatics* 11: 119.
33. Cantalapiedra, C. P., A. Hernández-Plaza, I. Letunic, P. Bork, and J. Huerta-Cepas. 2021. eggNOG-mapper v2: functional annotation, orthology assignments, and domain prediction at the metagenomic scale. *Mol. Biol. Evol.* 38: 5825–5829.
34. Harrison, O. J., N. Srinivasan, J. Pott, C. Schiering, T. Krausgruber, N. E. Ilott, and K. J. Maloy. 2015. Epithelial-derived IL-18 regulates Th17 cell differentiation and Foxp3$^+$ Treg cell function in the intestine. *Mucosal Immunol.* 8: 1226–1236.
35. Nowarski, R., R. Jackson, N. Gagliani, M. R. de Zoete, N. W. Palm, W. Bailis, J. S. Low, C. C. Harman, M. Graham, E. Elinav, and R. A. Flavell. 2015. Epithelial IL-18 equilibrium controls barrier function in colitis. *Cell* 163: 1444–1456.
36. Campbell, E., L. A. Hesser, and C. R. Nagler. 2021. B cells and the microbiota: a missing connection in food allergy. *Mucosal Immunol.* 14: 4–13.
37. Atarashi, K., T. Tanoue, M. Ando, N. Kamada, Y. Nagano, S. Narushima, W. Suda, A. Imaoka, H. Setoyama, T. Nagamori, et al. 2015. Th17 cell induction by adhesion of microbes to intestinal epithelial cells. *Cell* 163: 367–380.
38. Sun, L., and R. D. Ye. 2016. Serum amyloid A1: structure, function and gene polymorphism. *Gene* 583: 48–57.
39. Cheng, N., Y. Liang, X. Du, and R. D. Ye. 2018. Serum amyloid A promotes LPS clearance and suppresses LPS-induced inflammation and tissue injury. *EMBO Rep.* 19: e45517.
40. Tang, M. S., R. Bowcutt, J. M. Leung, M. J. Wolff, U. M. Gundra, D. Hudesman, L. B. Malter, M. A. Poles, L. A. Chen, Z. Pei, et al. 2017. Integrated analysis of biopsies from inflammatory bowel disease patients identifies SAA1 as a link between mucosal microbes with T_H17 and T_H22 cells. *Inflamm. Bowel Dis.* 23: 1544–1554.
41. Lee, J. Y., J. A. Hall, L. Kroehling, L. Wu, T. Najar, H. H. Nguyen, W. Y. Lin, S. T. Yeung, H. M. Silva, D. Li, et al. 2020. Serum amyloid A proteins induce pathogenic Th17 cells and promote inflammatory disease. [Published erratum appears in 2020 *Cell* 183: 2036–2039.] *Cell* 180: 79–91.e16.
42. Ohnmacht, C., J. H. Park, S. Cording, J. B. Wing, K. Atarashi, Y. Obata, V. Gaboriau-Routhiau, R. Marques, S. Dulauroy, M. Fedoseeva, et al. 2015. The microbiota regulates type 2 immunity through RORγt$^+$ T cells. *Science* 349: 989–993.
43. Sefik, E., N. Geva-Zatorsky, S. Oh, L. Konnikova, D. Zemmour, A. M. McGuire, D. Burzyn, A. Ortiz-Lopez, M. Lobera, J. Yang, et al. 2015. Individual intestinal symbionts induce a distinct population of RORγ$^+$ regulatory T cells. *Science* 349: 993–997.
44. Schulz, O., E. Jaensson, E. K. Persson, X. Liu, T. Worbs, W. W. Agace, and O. Pabst. 2009. Intestinal CD103$^+$, but not CX3CR1$^+$, antigen sampling cells migrate in lymph and serve classical dendritic cell functions. *J. Exp. Med.* 206: 3101–3114.
45. Bang, Y. J., Z. Hu, Y. Li, S. Gattu, K. A. Ruhn, P. Raj, J. Herz, and L. V. Hooper. 2021. Serum amyloid A delivers retinol to intestinal myeloid cells to promote adaptive immunity. *Science* 373: eabf9232.
46. Peterson, L. W., and D. Artis. 2014. Intestinal epithelial cells: regulators of barrier function and immune homeostasis. *Nat. Rev. Immunol.* 14: 141–153.
47. Ivanov, I. I., K. Atarashi, N. Manel, E. L. Brodie, T. Shima, U. Karaoz, D. Wei, K. C. Goldfarb, C. A. Santee, S. V. Lynch, et al. 2009. Induction of intestinal Th17 cells by segmented filamentous bacteria. *Cell* 139: 485–498.
48. Smole, U., N. Gour, J. Phelan, G. Hofer, C. Köhler, B. Kratzer, P. A. Tauber, X. Xiao, N. Yao, J. Dvorak, et al. 2020. Serum amyloid A is a soluble pattern recognition receptor that drives type 2 immunity. *Nat. Immunol.* 21: 756–765.
49. Yarur, A. J., M. A. Quintero, A. Jain, F. Czul, J. S. Barkin, and M. T. Abreu. 2017. Serum Amyloid A as a surrogate marker for mucosal and histologic inflammation in patients with Crohn's disease. *Inflamm. Bowel Dis.* 23: 158–164.
50. Bich, T. C. T., Q. L. Quoc, Y. Choi, E. M. Yang, H. K. T. Trinh, Y. S. Shin, and H. S. Park. 2022. Serum amyloid A1: a biomarker for neutrophilic airway inflammation in adult asthmatic patients. *Allergy Asthma Immunol. Res.* 14: 40–58.
51. Ozseker, F., S. Buyukozturk, B. Depboylu, D. Yilmazbayhan, E. Karayigit, A. Gelincik, S. Genc, B. Colakoglu, M. Dal, and H. Issever. 2006. Serum amyloid A (SAA) in induced sputum of asthmatics: a new look to an old marker. *Int. Immunopharmacol.* 6: 1569–1576.
52. Vatanen, T., A. D. Kostic, E. d'Hennezel, H. Siljander, E. A. Franzosa, M. Yassour, R. Kolde, H. Vlamakis, T. D. Arthur, A. M. Hämäläinen, et al.; DIABIMMUNE Study Group. 2016. Variation in microbiome LPS immunogenicity contributes to autoimmunity in humans. [Published erratum appears in 2016 *Cell* 165: 1551.] *Cell* 165: 842–853.
53. Spindler, M. P., S. Siu, I. Mogno, Z. Li, C. Yang, S. Mehandru, G. J. Britton, and J. J. Faith. 2022. Human gut microbiota stimulate defined innate immune responses that vary from phylum to strain. *Cell Host Microbe* 30: 1481–1498.e5.
54. Shah, C., R. Hari-Dass, and J. G. Raynes. 2006. Serum amyloid A is an innate immune opsonin for Gram-negative bacteria. *Blood* 108: 1751–1757.
55. McAlees, J. W., G. S. Whitehead, I. T. Harley, M. Cappelletti, C. L. Rewerts, A. M. Holdcroft, S. Divanovic, M. Wills-Karp, F. D. Finkelman, C. L. Karp, and D. N. Cook. 2015. Distinct *Tlr4*-expressing cell compartments control neutrophilic and eosinophilic airway inflammation. *Mucosal Immunol.* 8: 863–873.
56. Hammad, H., M. Chieppa, F. Perros, M. A. Willart, R. N. Germain, and B. N. Lambrecht. 2009. House dust mite allergen induces asthma via Toll-like receptor 4 triggering of airway structural cells. *Nat. Med.* 15: 410–416.
57. Ather, J. L., K. Ckless, R. Martin, K. L. Foley, B. T. Suratt, J. E. Boyson, K. A. Fitzgerald, R. A. Flavell, S. C. Eisenbarth, and M. E. Poynter. 2011. Serum amyloid A activates the NLRP3 inflammasome and promotes Th17 allergic asthma in mice. *J. Immunol.* 187: 64–73.
58. Sano, T., W. Huang, J. A. Hall, Y. Yang, A. Chen, S. J. Gavzy, J. Y. Lee, J. W. Ziel, E. R. Miraldi, A. I. Domingos, et al. 2015. An IL-23R/IL-22 circuit regulates epithelial serum amyloid A to promote local effector Th17 responses. [Published erratum appears in 2016 *Cell* 164: 324.] *Cell* 163: 381–393.
59. Liu, Y., M. Yang, L. Tang, F. Wang, S. Huang, S. Liu, Y. Lei, S. Wang, Z. Xie, W. Wang, et al. 2022. TLR4 regulates RORγt$^+$ regulatory T-cell responses and susceptibility to colon inflammation through interaction with *Akkermansia muciniphila*. *Microbiome* 10: 98.
60. Jia, Y. P., K. Wang, Z. J. Zhang, Y. N. Tong, D. Han, C. Y. Hu, Q. Li, Y. Xiang, X. H. Mao, and B. Tang. 2017. TLR2/TLR4 activation induces Tregs and suppresses intestinal inflammation caused by *Fusobacterium nucleatum* in vivo. *PLoS One* 12: e0186179.
61. Donaldson, G. P., M. S. Ladinsky, K. B. Yu, J. G. Sanders, B. B. Yoo, W. C. Chou, M. E. Conner, A. M. Earl, R. Knight, P. J. Bjorkman, and S. K. Mazmanian. 2018. Gut microbiota utilize immunoglobulin A for mucosal colonization. *Science* 360: 795–800.
62. Mazmanian, S. K., J. L. Round, and D. L. Kasper. 2008. A microbial symbiosis factor prevents intestinal inflammatory disease. *Nature* 453: 620–625.
63. Mills, R. H., P. S. Dulai, Y. Vázquez-Baeza, C. Sauceda, N. Daniel, R. R. Gerner, L. E. Batachari, M. Malfavon, Q. Zhu, K. Weldon, et al. 2022. Multi-omics analyses of the ulcerative colitis gut microbiome link *Bacteroides vulgatus* proteases with disease severity. *Nat. Microbiol.* 7: 262–276.